An Increase in Epithelial Cell Apoptosis Is Associated with Chronic Intestinal Nematode Infection[▽]

Laura J. Cliffe,[1][†] Christopher S. Potten,[2] Catherine E. Booth,[2] and Richard K. Grencis[1][*]

Faculty of Life Sciences, Michael Smith Building, University of Manchester, Manchester M13 9PT, United Kingdom,[1] and Epistem Limited, Incubator Building, 48 Grafton Street, Manchester M13 9XX, United Kingdom[2]

It is well established that homeostasis of the intestinal epithelium becomes dysregulated during gastrointestinal helminth infection and is under immune control. An increase in both enterocyte proliferation and the subsequent generation of crypt hyperplasia are hallmarks of chronic infection with *Trichuris muris*, a large intestinal dwelling nematode. The effect of this parasitic infection on apoptosis induction in the large intestine and its regulation has been neglected. To address this, mice of resistant and susceptible phenotypes were infected with different doses of *T. muris*, and the levels of epithelial cell apoptosis were determined. It is clear that apoptosis is induced during chronic *T. muris* infection. This occurs mainly at the base of the cecal crypt, within the stem cell region. The level of apoptosis induced is independent of worm number, suggesting that it is not a consequence of worm-induced damage but rather a mechanism for controlling cell number within the crypt. Neutralization of both gamma interferon and tumor necrosis factor alpha caused a significant reduction in the levels of apoptosis, showing that proinflammatory cytokines generated in response to chronic infection play an important role in apoptosis induction in this system. It is proposed that the generation of proinflammatory cytokines during chronic *T. muris* infection may play a positive role, by promoting intestinal epithelial cell apoptosis, to counter infection-induced epithelial hyperplasia.

Gastrointestinal helminths infect over 1 billion people worldwide. Although rarely causing death, such diseases are associated with high levels of morbidity and bear a high economic burden within areas where infection is endemic.

Trichuris muris, a natural intestinal parasite of mice, has been extensively utilized as a laboratory model for the study of human whipworm *Trichuris trichiura*. Transmission of *T. muris* occurs via a direct feco-oral route through the ingestion of infective eggs. The intestinal epithelium forms an intimate host-parasite interface, as upon ingestion of infective eggs larvae hatch and penetrate the epithelium, forming syncytial tunnels within which they reside throughout infection.

Immune-mediated expulsion of intestinal dwelling nematodes can involve the interplay between CD4$^+$ T cells and the gut epithelium. Resistance and susceptibility to *T. muris* infection are tightly associated with a polarization in the T helper (TH) cytokine response generated. Resistance is characterized by the production of TH2 cytokines, namely, interleukin-4 (IL-4), IL-5, IL-9, and IL-13 (5, 8, 15, 17). Indeed, IL-13 regulation of intestinal epithelial cell turnover is an important component of the host protective (13) response. Resistant animals are capable of parasite expulsion before worms reach maturity. Susceptible animals mount a TH1 response, generating high levels of gamma interferon (IFN-γ), IL-12, and IL-18 (6, 7, 15, 27). Such animals fail to expel the parasite, and infection progresses to chronicity.

Dysregulation of epithelial homeostasis is apparent during insult to the intestine with a number of bacterial, viral, protozoan, and helminth infections (9, 10, 19, 25, 46, 49). The development of a marked crypt cell hyperplasia coupled with villus atrophy are typical of such infections. Proinflammatory cytokine production plays a key role within the intestinal environment during insult and/or disease. Indeed, both IFN-γ and tumor necrosis factor alpha (TNF-α) levels are elevated during Crohn's disease and are thought to be important in disease pathogenesis (33, 36, 53).

Animals that are susceptible to *T. muris* infection mount a TH1 immune response, regardless of whether a high- or a low-dose infection is given. Susceptible animals fail to expel the parasite, and therefore infection becomes chronic. During chronic *T. muris* infection, a TH1 immune response can be detected not only in the draining lymph node but also in the gut tissue. It has been demonstrated that high levels of IFN-γ within the intestine drives the development of pathology during chronic *T. muris* infection. The neutralization of IFN-γ during infection causes a reduction in both crypt length and epithelial cell proliferation (2), identifying a key role for IFN-γ nematode associated alteration in epithelial architecture.

The pleiotropic cytokine TNF-α can promote inflammation through leukocyte recruitment and activation, as well as enhancing the secretion of other proinflammatory cytokines such as IL-1 and IL-6 (45). Moreover, the levels of TNF-α are increased after *T. muris* infection (1). TNF-α can induce epithelial cell apoptosis in vivo (23) and has been suggested to play an integral role in the development of pathology associated with inflammatory bowel disease and graft-versus-host disease (GVHD) (11).

This study defines for the first time that apoptosis is induced after chronic *T. muris* infection and importantly that the pro-

* Corresponding author. Mailing address: Michael Smith Building, University of Manchester, Oxford Road, Manchester M139PT, United Kingdom. Phone: 44 161 2755240. Fax: 44 161 2751498. E-mail: richard .k.grencis@manchester.ac.uk.
† Present address: Department of Biochemistry and Molecular Biology, Life Sciences, University of Georgia, Athens, GA 30602.

duction of the proinflammatory cytokines TNF-α and IFN-γ play a role in infection associated programmed cell death. Given that an excess of one billion people harbor chronic helminth infection, worm-induced perturbation of the epithelium and its resultant impact on gut function bears important implications for how and what we consider as normal or "steady state" when regarding intestinal physiology and concerning immunocompetence at mucosal surfaces.

MATERIALS AND METHODS

Animals. Male AKR, BALB/c, and C57BL/6 were obtained from Harlan-Olac, Ltd., United Kingdom. C.B-17$^{SCID/SCID}$ SCID, TNF p55$^{-/-}$, and p75$^{-/-}$ mice were from Jackson Laboratories. All mice were 6- to 8-week-old males. All experiments were performed under the regulations of the Home Office Scientific Procedures Act (1986).

Parasite. $T.$ $muris$ was maintained as previously described (52). Mice were infected by oral gavage to give either 200 to 300 embryonated eggs (high level) or 10 to 20 eggs (low dose) in double-distilled H$_2$O. Worm burdens were assessed at various time points postinfection by methods described previously (16).

Purification and administration of anti-IFN-γ MAb. Rat immunoglobulin G1 monoclonal antibody (MAb) XMG1.6 (anti-IFN-γ) and GL113 (isotype control MAb) were purified from supernatants by passage over a protein G-Sepharose column and concentration by using Centricon Centriprep tubes.

The MAbs were administered at 1 mg per 200 μl of phosphate-buffered saline by intraperitoneal injection. Injections were given every 4 days starting at day −2 to day 42 postinfection (p.i.).

Tissue preparation. Cecum samples were removed and flushed out by using saline. Samples were fixed intact in Carnoy fixative for 30 min prior to storage in 70% ethanol. Tissues were prepared by using the gut bundle technique (40). Tissues were then paraffin embedded by using standard histological techniques. Two nonserial 3-μm sections were mounted per slide and stained with hematoxylin and eosin.

Detection of apoptotic cells. Sections were stained with hematoxylin and eosin to allow the visualization of apoptotic cells. Such cells are detected on the basis of their morphology by using light microscopy, a method that has been used extensively (28, 29, 35, 41). Typically, apoptotic cells appear pink and circular, with a crescent-shaped nucleus, and are bubbled up out of the plain of focus. Tunnel labeling is another method that has can be used to detect apoptosis in the intestinal epithelium. However, this technique is prone to false-positive and false-negative results compared to morphological assessment, as well as failing to distinguish between DNA cleaved by apoptosis and DNA fragments cleaved by other processes (39). For the purpose of this investigation, therefore, morphological analysis was deemed the most reliable method to use.

Levels of epithelial cell proliferation. Groups of four mice were injected intraperitoneally with 10 mg of bromodeoxyuridine (BrdU; Sigma, Poole, United Kingdom) 40 min prior to sacrifice. All animals were killed at the same time within and between experiments to minimize any differences in proliferation attributable to variation in circadian rhythm. Detection of nuclei that had incorporated BrdU was performed by immunohistochemistry using a monoclonal anti-BrdU antibody (Mas 250b; Harlan Serum Laboratories, Loughborough, United Kingdom) as described previously (13). Sections were analyzed by scoring 50 cecal crypts per mouse with four mice per group.

Scoring. Full-length longitudinal sections of crypts were selected for analysis. All histological sections were scored blindly. The scoring commenced with the cell at the midpoint at the base of the crypt, which was designated as position 1, and continued until the crypt-crypt table was reached. For each mouse 50 crypts were scored, with four mice in each group. This method of scoring allows the generation of statistically valid results (41) and was used to determine the levels of apoptotic and proliferating cells. In this way both the position and the overall numbers of apoptosing cells in the cecum can be determined.

Determination of the levels of IFN-γ and IL-12p40 secretion. Mesenteric lymph node cells (MLNC) were removed, cultured, and restimulated for 24 h under conditions previously described (8). Sandwich enzyme-linked immunosorbent assay was performed to analyze cytokine levels, using pairs of MAbs (IFN-γ R46A2 and XMG1.2 and IL-12 C15.6 and C17.8; BD Pharmingen, San Diego, CA). The amount of each cytokine was determined by reference to commercially available recombinant murine standards. The sensitivity of the assay was determined by taking the mean plus three standard deviations of 16 control wells containing medium only.

Detection of TNF-α and IFN-γ in the cecum. The presence of IFN-γ and TNF-α in whole gut was determined by reverse transcription-PCR. Briefly, tissue samples were snap-frozen in TRIzol (Gibco, United Kingdom), and the RNA isolated was reverse transcribed by using IMPROMII (Promega). The primers used were the IFN-γ sense (5′- AGCTCTTCCTCATGGCTGTTTC-3′) and antisense (5′-ATGTTGTTGCTGATGGCCTGA-3′) primers and the TNF-α sense (5′-TCTTCTCATTCCTGCTTGTGG-3′) and antisense (5′- GACAACC TGGGAGTAGACAAGGT-3′) primers. For each reaction, cDNA (0.5 μg) was used in a 25-μl PCR.

Measurement of crypt length and epithelial area. The area of the epithelium was assessed by using a computer-assisted Zeiss Axiohome microscope system to mark around the area of interest. Analysis was performed on hematoxylin-and-eosin-stained sections, at four mice per group, with three to four circumferences per mouse. The circumference of the lumen was subtracted from the circumference of the muscularis (which runs under the base of the crypts) to give the area of the epithelium. Individual crypt lengths were determined by using the same system, selecting well orientated crypts, and measuring from the base of the crypt to the lumen. Fifty crypts per mouse were measured, with four mice per group.

Statistical analysis. Statistical analysis was performed by using a one-way analysis of variance (ANOVA) with a Tukey test to determine the significance for multiple comparisons. Analysis was performed by using the Aabel statistic program. The Student t test was also used for analysis. For both ANOVA and Student t tests, P values of <0.05 were considered statistically significant.

RESULTS

Both epithelial cell apoptosis and proliferation are elevated during chronic nematode infection. Worm expulsion kinetics following a high-dose infection of susceptible AKR and resistant BALB/c mice displayed the expected trend, with BALB/c mice expelling all parasites by day 21 p.i., whereas in AKR mice infection developed to patency, with worms still present at day 42 p.i. (Fig. 1A).

Apoptosis was assessed during a time course of infection, with animals sacrificed at days 14, 21, and 42 p.i. Apoptosis levels in naive animals were also assessed for the purpose of comparison (Fig. 1B). It is clear that the percentage of intestinal epithelial cells undergoing apoptosis in the BALB/c mouse never exceeds the baseline levels seen in naive animals. However, in susceptible AKR mice, a significant elevation in apoptosis is detected at day 42 p.i., once infection has reached chronicity ($P < 0.0007$) (Fig. 1B, C, and D). The levels of epithelial cell proliferation were determined by using BrdU incorporation to identify cells in S phase of the cell cycle. In accordance with previous studies (2, 13), the levels of proliferation were elevated in chronically infected animals (Fig. 1E and F). This temporal association of proliferation and apoptosis highlights that chronic nematode infection can have profound effects on epithelial homeostasis, the dysregulation of which results in the generation of crypt hyperplasia (Fig. 1G).

The induction of epithelial cell apoptosis is not due to physical damage elicited by the parasite. In order to investigate whether the elevation in the numbers of cells apoptosing in the intestine is simply a consequence of the physical damage elicited by the parasites, the levels of apoptosis observed after a low-dose infection were investigated. Mice were infected with 10 to 20 infective $T.$ $muris$ eggs. Worm burdens and apoptosis levels were assessed at day 42 p.i. Low-dose infection established in AKR mice, with the mean worm burden of 13 ± 2.16 compared to 89.6 ± 19.87 during a high-dose infection (Fig. 2A). If the apoptosis seen was a simple response to damage caused by the physical presence of the parasite, we would expect to see much higher levels of apoptosis in animals where worm numbers were greater. However, there was no significant
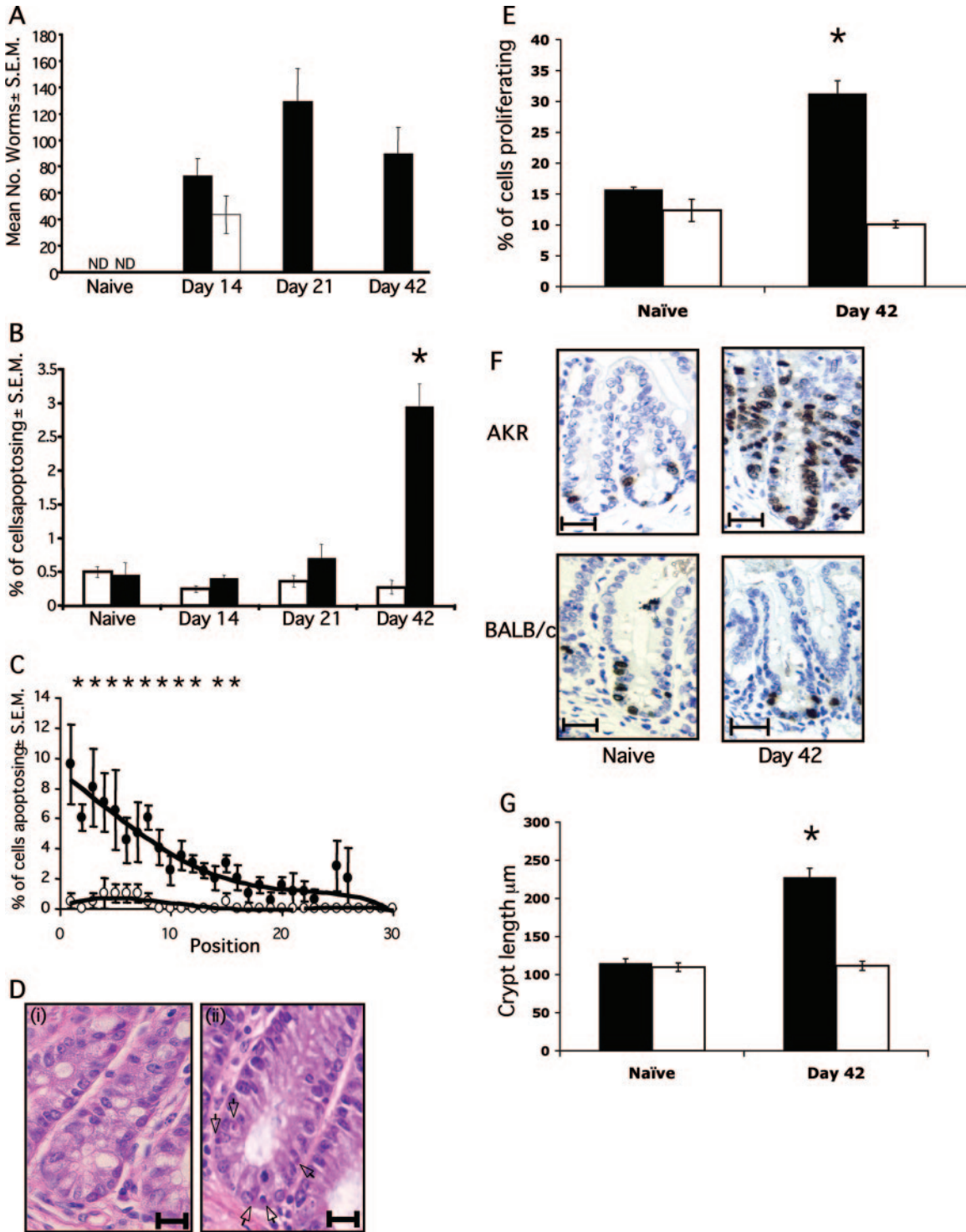
FIG. 1. Levels of apoptosis during *T. muris* infection. (A) AKR (■) and BALB/c (□) mice were infected with 200 *T. muris* eggs by oral gavage. Worm burdens were assessed at various time points postinfection. ND, not detected. (B) The levels of apoptosis were assessed at days 14, 21, and 42 p.i. in AKR (■) and BALB/c (□) mice. Apoptotic cells were identified by their morphology on sections stained with hematoxylin and eosin. Four mice per group were scored, with 50 crypts per mouse. (C) Location of epithelial cells within the crypt. The percentage of cells apoptosing at each position was assessed. Symbols: ●, AKR mice; ○, BALB/c mice. A "0" value is the base of the crypt, and "30" is the lumen. (Di) Absence of apoptosing cells in naive AKR cecum. Scale bar, 20 μm. (Dii) Apoptosing cells in AKR ceca at day 42 p.i. (black arrows). Scale bar, 15 μm. (E) Epithelial cell proliferation was assessed by BrdU incorporation in AKR mice (■) and BALB/c mice (□). (F) Histology of BrdU staining in the cecal epithelium. Scale bar, 30 μm. BrdU-positive cells are stained brown. (G) Crypt length in AKR mice (■) and BALB/c mice (□). Each datum point represents the mean of four animals ± the standard error of the mean (SEM). *, the Student *t* test showed a statistically significant increase in AKR mice versus BALB/c mice ($P < 0.001$).
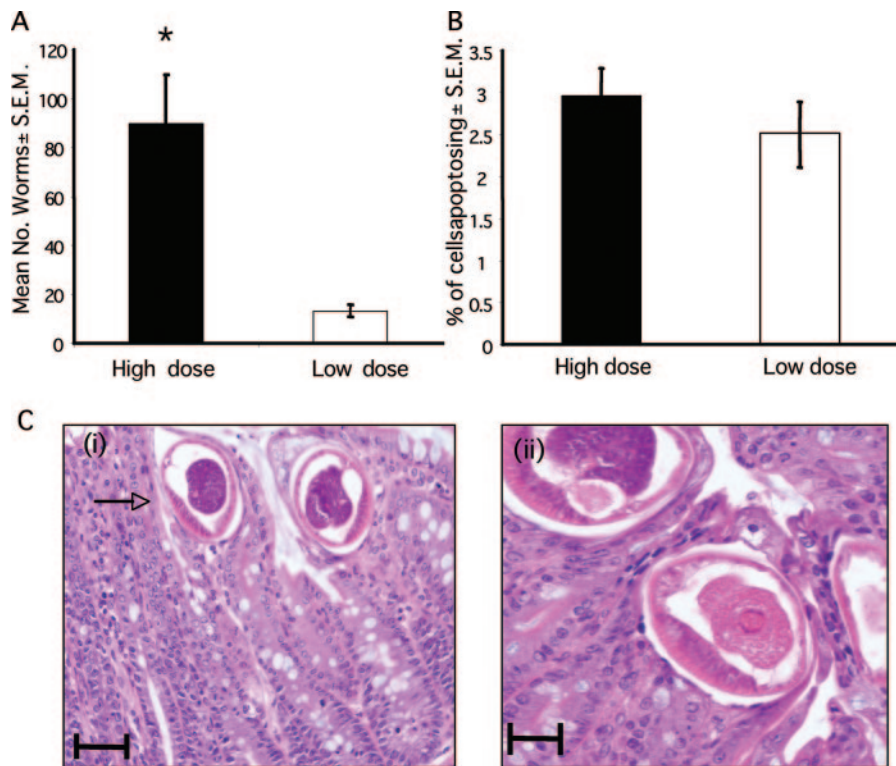
FIG. 2. Apoptosis during low-dose *T. muris* infection. AKR mice were given either a low-dose (□) *T. muris* infection (25 eggs) or a high-dose (■) infection (200 eggs). (A) Worm burdens were assessed at day 42 p.i. (B) Apoptosis levels were assessed at day 42 p.i. Each bar represents the mean of four animals ± the S.E.M. ∗, the Student *t* test reveals a statistically significant difference between the two groups ($P < 0.001$). (Ci) Mature worms in epithelial tunnel at day 42 p.i. The arrow indicates the anterior end. Scale bar, 50 μm. (Cii) Image of worm showing epithelial tunnel surrounding the parasite, along with an absence of apoptosing cells in close proximity. Scale bar, 25 μm.

difference between the percentage of cells undergoing apoptosis in the ceca of animals given low- or high-dose infections (Fig. 2B), despite the highly significant difference in worm burdens (Fig. 2A) ($P < 0.0001$). It is also interesting that the cells undergoing apoptosis were located near the base of the crypt, away from the worms, which are embedded within tunnels near the epithelial surface at this late stage of infection (Fig. 1C and D and Fig. 2C). Indeed, no apoptosis could be seen in the epithelial tunnels surrounding the worms (Fig. 2C). Again, this suggests that worm-induced damage is not directly responsible for the high levels of apoptosis seen with chronic infection. This finding is consistent with studies by Li et al. (30), who demonstrate that *Trichinella spiralis* fails to induce epithelial cell apoptosis in vitro.

TNF-α can stimulate epithelial cell apoptosis both in vivo (11) and in vitro (11, 20, 43). Furthermore, IFN-γ can induce apoptosis (36, 53). In an attempt to determine what factors might be contributing to the increase in apoptosis levels seen in the large intestine during chronic helminth infection, the role of TNF-α and IFN-γ were investigated. Both are produced by permissive hosts (1, 15), which develop a TH1-like intestinal colitis (independent of dose) and are therefore feasible candidates for the induction of apoptosis in this system. Indeed, the immune response to *T. muris* is well characterized. Elevated levels of IFN-γ, IL-12, IL-18, and TNF-α are detected in both the MLNC and the intestinal mucosa of susceptible animals (2,

13, 15, 27). Moreover, chronic infection is associated with enhanced leukocyte infiltration into the gut (31).

TNF-α levels are increased in both the MLNC and the gut of animals susceptible to *T. muris*. The expression of TNF-α in both susceptible (AKR) and resistant (BALB/c) mice was assessed in the cecum through a time course of infection. AKR mice demonstrated enhanced mRNA levels for TNF-α at days 21 and 42 p.i. compared to BALB/c mice. (Fig. 3Ai). Moreover, during the peak of cytokine production (day 21 p.i.) the message for TNF-α was significantly upregulated in the mesenteric lymph node of susceptible AKR mice compared to resistant mice (Fig. 3Aii). Furthermore, low-dose infection of C57BL/6 mice also results in an elevation in the levels of TNF-α in the cecum (Fig. 3Aiii).

p55$^{-/-}$ and p75$^{-/-}$ mice display significant differences in levels of apoptosis during infection. To test the hypothesis that TNF-α may contribute to the elevation in apoptosis during chronic infection, we infected mice deficient in either the p55 or the p75 TNF receptor (TNFR). The p55 receptor is associated with a death domain (38) and is thought to be the main TNFR associated with apoptosis induction (3). However, it is clear that the induction of apoptosis through the p75 receptor can also occur, although the pathways are thought to occur independently of each other (21, 22, 50). Gene-deficient animals received a high-dose *T. muris* infection that progressed to chronicity. Since wild-type (WT) animals are resistant to such
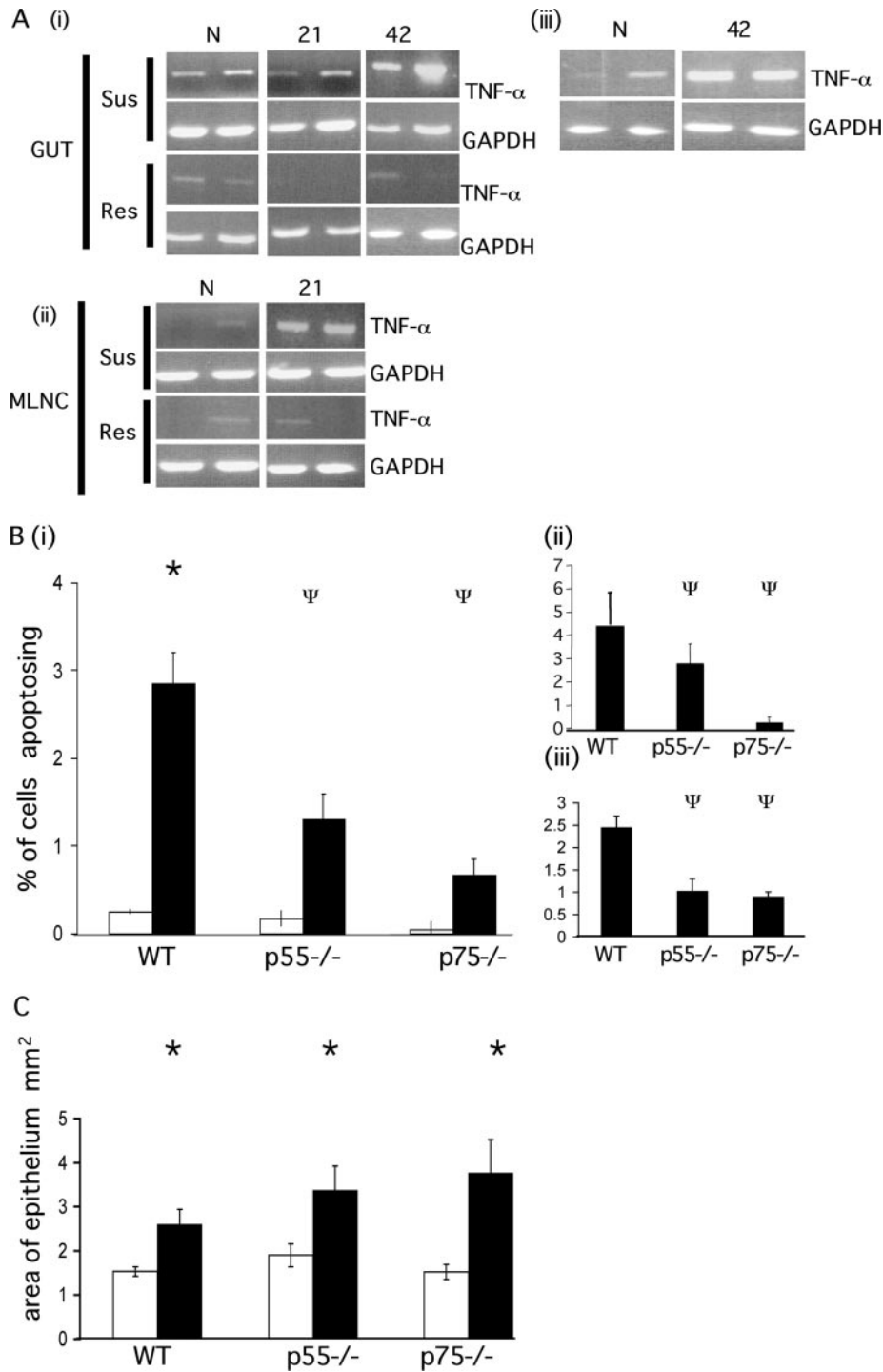
FIG. 3. Apoptosis in TNFR-deficient animals during chronic *T. muris* infection. (A) The expression of TNF-α in the gut (i) and MLNC (ii) of AKR (susceptible) and BALB/c (resistant) mice was assessed by PCR at various times p.i. (iii) TNF-α expression in the gut tissue of C57BL/6 mice following low-dose infection was assessed by PCR. GAPDH (glyceraldehyde-3-phosphate dehydrogenase) levels were assessed as a control transcript. N, naive animals; 21, 21 days p.i.; 42, 42 days p.i. (B) p55$^{-/-}$, p75$^{-/-}$, and WT mice were infected with *T. muris*. The levels of apoptosis were assessed at day 42 p.i. and are expressed as the total percentage of cells apoptosing (i) and as the percentage of cells apoptosing in the base of the crypt (positions 1 to 4) (ii) and higher up the crypt axis (positions 11 to 30) (iii). Bars: □, naive animals; ■, infected animals. (C) The area of the epithelium was assessed at day 42 p.i. Bars: □, naive animals; ■, infected animals. Each datum point represents the mean of four animals ± the SEM. *, ANOVA and Tukey tests showed a statistically significant increase in infected versus naive animals ($P < 0.001$); Ψ, ANOVA and Tukey tests showed a statistically significant reduction in gene-deficient mice compared to WT mice ($P < 0.001$).

a high level of infection, they were given a low-dose level infection. This renders animals susceptible to infection, allowing chronic infection to develop. Therefore, both gene-deficient and WT animals were susceptible to infection with *T. muris*. Despite infection reaching chronicity in all three mouse strains, there were significant differences in the levels of apoptosis detected between each strain (Fig. 3B). Infected WT mice displayed a significant increase in the levels of apoptosis versus naive mice (F, 22.95; $P < 0.001$) (Fig. 3Bi), but both p55 and p75$^{-/-}$ animals show no significant increase. Moreover, the levels of apoptosis in infected p55$^{-/-}$ and p75$^{-/-}$ animals are significantly reduced compared to WT ($P > 0.001$). Interestingly, p75$^{-/-}$ display reduced levels of apoptosis in comparison with p55$^{-/-}$, despite p55 being the classical receptor associated with apoptosis. The distribution of apoptosing cells within the crypt unit also differs between p55 and p75 mice. It would appear that signaling through p75 induces apoptosis in the base in the base of the crypt (Fig. 3Bii), whereas p55-induced apoptosis occurs further up the crypt, in cells that are more differentiated (Fig. 3Biii). These data suggest a distributional separation of both receptors within the crypt unit. The area of epithelium was determined to indicate the level of hyperplasia and therefore dysregulation of intestinal homeostasis. It is apparent from Fig. 3C that the area of epithelium is increased in p55$^{-/-}$ and p75$^{-/-}$ animals over WT mice. Moreover, the elevation in crypt hyperplasia seen in p75$^{-/-}$ is slightly greater than that in p55$^{-/-}$ mice, correlating with a larger reduction in epithelial cell apoptosis in the stem cell region. Ultimately, the failure of these mice to upregulate epithelial cell apoptosis to levels displayed by WT animals, despite the persistence of *T. muris* indicates that TNF-α enhances epithelial cell apoptosis during chronic helminth infection. Whether this is through the direct ligation of an epithelial cell specific receptor, or indirectly through the recruitment of inflammatory cells/enhanced inflammatory mediator production remains to be determined.

Neutralization of IFN-γ in SCID mice inhibits *T. muris*-associated epithelial cell apoptosis without altering the outcome of infection. The data presented thus far indicate that the elevated levels of TNF-α in the intestine may play an important role in the induction of epithelial cell apoptosis during chronic *T. muris* infection. Coincident with TNF-α expression, susceptible animals also demonstrate elevated levels of IFN-γ in the cecal mucosa, as has been documented for a high-dose infection in AKR mice (13, 2) and during low-dose infection in C57BL/6 mice (Fig. 4A). SCID mice are deficient in B cells and T cells and therefore have no adaptive immunity. It has previously been shown that the neutralization of IFN-γ in SCID mice can reduce the levels of proliferating cells in the intestine during *T. muris* infection (2), suggesting a role for IFN-γ in the maintenance of epithelial homeostasis. Although the source of this IFN-γ remains unknown, it has been suggested to be derived from NK cells, macrophages, and myeloid cells (42, 54). Moreover, it has been shown that IFN-γ can induce epithelial cell apoptosis (11, 43, 55). To determine whether IFN-γ played a role in epithelial cell apoptosis during *T. muris* infection, the cytokine was neutralized in SCID mice for the duration of infection (42 days). SCID mice were utilized for the present study since neutralization of IFN-γ in immunocompetent animals causes a switch to a TH2 immune response and subsequent parasite expulsion. Therefore, the use of SCID
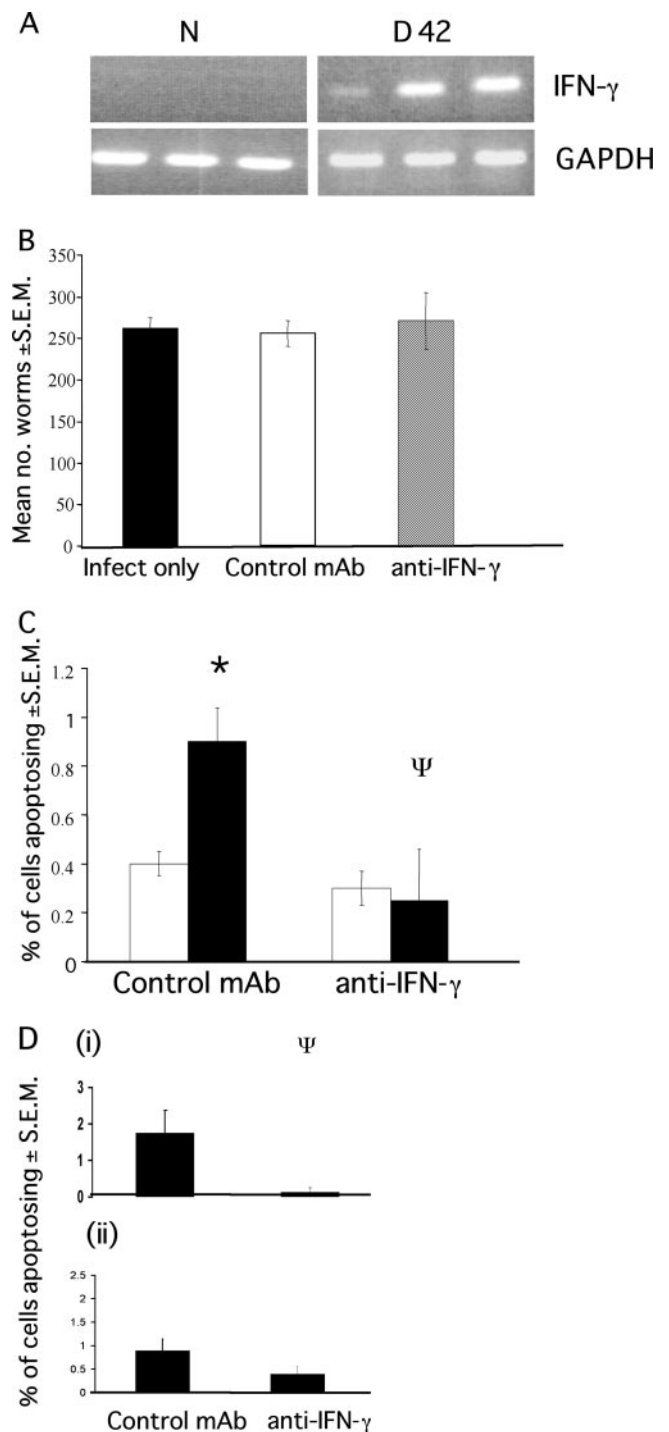

FIG. 4. Apoptosis levels in SCID mice after neutralization of IFN-γ. SCID mice received either anti-IFN-γ (XMG1.6) or a control MAb GL113 at 1 mg/injection every 4 days for the duration of infection. (A) IFN-γ is expressed in the cecum during low-dose infection in C57BL/6 mice (B) Worm recovery from SCID mice treated with either anti-IFN-γ or control MAb. Each value represents a mean of four animals ± the SEM. (C) The levels of apoptosis were assessed at day 42 p.i. (□, naive mice; ■, infected mice). (D) The position of apoptosing cells in the ceca of infected animals was assessed in the base of the crypt (cell positions 1 to 4) (i) and higher up the crypt (cell positions 11 to 15) (ii). Each value represents the mean of four animals ± the SEM. ∗, ANOVA and Tukey tests revealed a statistically significant difference between naive and infected animals and between control and anti-IFN-γ-treated mice ($P < 0.01$).
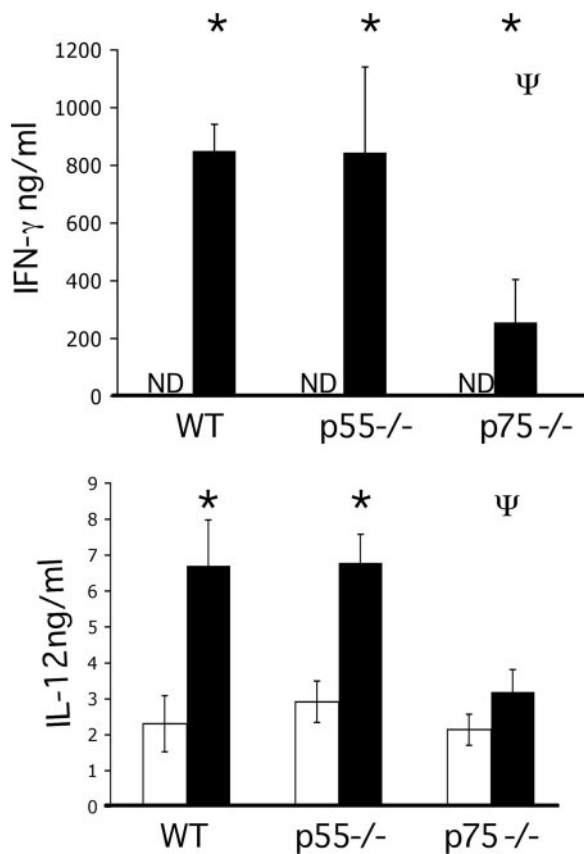
FIG. 5. The levels of IFN-γ and IL-12 secreted by MLNC isolated at day 42 p.i. were determined in WT, p55$^{-/-}$, and p75$^{-/-}$ animals by ELISA. Each value represents the mean of four animals ± the SEM. ∗, ANOVA and the Tukey test showed a statistically significant increase in infected versus naive animals; Ψ, statistically significant difference between WT and gene-deficient mice ($P < 0.05$). Bars: □, naive animals; ■, infected animals. ND, not detected. All cytokine levels shown are over the limit of detection.

mice allows the effect of IFN-γ neutralization on apoptosis to be investigated during chronic infection. Indeed, all treatment groups remained susceptible to infection (Fig. 4B). Despite the high worm numbers in all of these animals, the levels of apoptosis were, as with the TNFR$^{-/-}$ animals, much lower than those detected in immunocompetent C57BL/6 and AKR mice at day 42 p.i. (Fig. 1B and 3B). Mice in which IFN-γ was neutralized show a significant reduction in apoptosis levels compared to control treated animals (F, 5.92; $P < 0.01$) (Fig. 4C and D). This suggests that IFN-γ plays a contributory role in the development of cecal epithelial cell apoptosis during infection. Interestingly, the neutralization of IFN-γ appeared to cause the greatest reduction in the apoptosis of cells positioned at the base of the crypt (Fig. 4Di). These cells also show the greatest reduction in proliferation after IFN-γ neutralization (2).

The levels of IFN-γ produced by MLNC from TNFR$^{-/-}$ animals shows WT, p55, and p75$^{-/-}$ mice all make the characteristic TH1 response with elevated levels of IFN-γ and IL-12 (Fig. 5A and B) and low levels of TH2 cytokines (data not shown). However, despite the persistence of infection in all three strains, the production of parasite specific IFN-γ was

significantly reduced in p75$^{-/-}$ animals compared to both WT and p55$^{-/-}$ mice. This correlates with the lower levels of apoptosis seen in the TNF p75$^{-/-}$ animals.

DISCUSSION

We show here for the first time that chronic *T. muris* infection is associated with an elevation in the level of epithelial cell apoptosis in the large intestine. Moreover, the demonstration that both TNF-α and IFN-γ play a role in the development of apoptosis in a naturally occurring model of epithelial cell apoptosis is novel.

The basal levels of apoptosis in the colon are low compared to the small intestine, and this is thought to be influenced in part by the high levels of the antiapoptotic molecule BCL-2 in the bases of the crypts. Certainly, the finding that infection induces apoptosis within the epithelial cells positioned at the base of the crypt is surprising.

It is evident that the upregulation of apoptosis is not merely a consequence of physical damage to the intestine induced by worm burrowing, since both low- and high-dose infections result in equivalent levels of apoptosis. This elevation in apoptosis is only detected during chronic infection, despite the active burrowing of larvae through the intestinal epithelium during early infection. Moreover, there exists spatial separation between the worms and the apoptosis. During chronic infection the majority of apoptosing cells are located at the base of the crypt, distant from the parasite, the anterior end of which is embedded with in epithelial tunnels near the gut lumen.

The data presented here suggest that the increase in apoptosis is a product of the host response to chronic infection rather than infection per se. Apoptosis is detected only when infection reaches chronicity, at which point high levels of proinflammatory cytokines are detected in the intestinal mucosa of infected animals (Fig. 3 and 4). Infection of TNF-α receptor-deficient animals revealed TNF-α signaling to play a role in the induction of intestinal apoptosis associated with chronic infection, with both p55$^{-/-}$ and p75$^{-/-}$ animals demonstrating a significant reduction in apoptosis levels compared to the WT strain. Signaling through either the p55 or the p75 receptor alone shows a reduction in apoptosis levels. This suggests that signaling through both receptors is important for optimal apoptosis induction. This has been demonstrated in in vitro experiments with IEC-6 cells, where stimulation through both p55 and 75 resulted in enhanced apoptosis (32).

Although SCID animals lack B and T cells, it is assumed that other sources of both IFN-γ and TNF-α do exist. After in vivo depletion of IFN-γ, we see a complete loss of apoptosis. TNF-α fails to act in a compensatory manner in these animals (although the levels may be subthreshold). It is interesting that the levels of apoptosis in SCID animals with or without treatment are much lower than those seen during chronic infection in an immunocompetent animal. This suggests that during chronic *T. muris* infection T-cell-derived cytokines may be important in mediating the apoptosis seen during infection of immunocompetent mice. Activated T cells have been identified as key players in driving the mucosal pathology associated with a number of inflammatory diseases of the intestine, including GVHD, celiac disease, and the inflammation seen during anti-

CD3 treatment (4, 32, 34, 51). Interestingly, the pathology associated with GVHD bears striking similarities with that seen during gut nematode infection. As with *T. muris* infection, the development of both crypt hyperplasia and epithelial cell apoptosis has been reported in GVHD (24, 37, 47, 48). Moreover, a role for both IFN-γ and TNF-α in the development GVHD-related pathology is clear (12, 14, 48). Indeed, the neutralization of TNF-α inhibits the development of GVHD-associated epithelial cell apoptosis (12, 47).

Many questions still exist regarding the mechanism of action for both TNF-α and IFN-γ in this system. Whether the cytokines act through direct ligation of receptors on epithelial cells remains to be determined. It is certainly possible that TNF-α may promote apoptosis in an indirect manner by enhancing the production of IFN-γ and by the recruitment of inflammatory cells into the intestinal microenvironment. The release of free radicals and inflammatory mediators by infiltrating cells can induce oxidative stress, DNA damage, and epithelial cell apoptosis. The synergistic nature of these cytokines should not be ignored; a number of studies have demonstrated that IFN-γ and TNF-α can act together to inhibit cell growth (18). Moreover, it has been shown that that IFN-γ can upregulate TNFR expression (44).

The elevated level of apoptosis found in the gut during chronic *T. muris* infection is coincident with a profound crypt cell hyperplasia and epithelial cell proliferation (Fig. 1, 3, and 4) (2, 13). It is reasonable to suggest that the induction of apoptosis is acting in favor of the host to regulate crypt size. Certainly, there must exist a crypt length, which when exceeded will be deleterious for the host. Apoptosis would, therefore, be an effective regulatory mechanism to bring about homeostasis at the epithelial level. Indeed, apoptosis occurs predominantly near the base of the crypts, in the stem cell compartment. Ultimately, death of a stem cell would have much more profound effect on limiting crypt size than would death of a differentiated enterocyte. Whether the induction of apoptosis in this compartment occurs during chemical insult or chronic inflammation is difficult to determine from the literature, since positional analysis of apoptosing cells rarely performed. However, it is feasible to suggest that this mechanism of crypt cell regulation may operate in a number of inflammatory conditions to curb the development of excessive hyperplasic change.

Taken together, these data support a "positive" role for proinflammatory cytokines in the induction of apoptosis at the epithelial level by inducing intestinal homeostasis in an attempt to control the dysregulation of epithelial architecture seen during *T. muris* infection. Although the induction of both proinflammatory cytokines and apoptosis are typically thought to be detrimental during intestinal colitis, they may in fact act in a host-protective manner during chronic *T. muris* infection by controlling the level of homeostatic dysregulation in the gut. Ultimately, this is beneficial for both host and parasite.

REFERENCES

1. **Artis, D., N. E. Humphreys, A. J. Bancroft, N. J. Rothwell, C. S. Potten, and R. K. Grencis.** 1999. Tumor necrosis factor alpha is a critical component of interleukin 13-mediated protective T helper cell type 2 responses during helminth infection. J. Exp. Med. **190:**953–962.
2. **Artis, D., C. S. Potten, K. J. Else, F. D. Finkelman, and R. K. Grencis.** 1999. *Trichuris muris:* host intestinal epithelial cell hyperproliferation during chronic infection is regulated by interferon gamma. Exp. Parasitol. **92:**144–153.
3. **Ashkenazi, A., and V. M. Dixit.** 1998. Death receptors: signaling and modulation. Science **281:**1305–1308.
4. **Baker, M. B., N. H. Altman, E. R. Podack, and R. B. Levy.** 1996. The role of cell-mediated cytotoxicity in acute GVHD after MHC-matched allogeneic bone marrow transplantation in mice. J. Exp. Med. **183:**2645–2656.
5. **Bancroft, A. J., D. Artis, D. D. Donaldson, J. P. Sypek, and R. K. Grencis.** 2000. Gastrointestinal nematode expulsion in IL-4 knockout mice is IL-13 dependent. Eur. J. Immunol. **30:**2083–2091.
6. **Bancroft, A. J., K. J. Else, N. E. Humphreys, and R. K. Grencis.** 2001. The effect of challenge and trickle *Trichuris muris* infections on the polarisation of the immune response. Int. J. Parasitol. **31:**1627–1637.
7. **Bancroft, A. J., K. J. Else, J. P. Sypek, and R. K. Grencis.** 1997. Interleukin-12 promotes a chronic intestinal nematode infection. Eur. J. Immunol. **27:**866–870.
8. **Bancroft, A. J., A. N. McKenzie, and R. K. Grencis.** 1998. A critical role for IL-13 in resistance to intestinal nematode infection. J. Immunol. **160:**3453–3461.
9. **Barker, I. K.** 1975. Intestinal pathology associated with *Trichostrongylus colubriformis* infection in sheep: histology. Parasitology **70:**165–171.
10. **Boshuizen, J. A., J. H. Reimerink, A. M. Korteland-van Male, V. J. van Ham, M. P. Koopmans, H. A. Buller, J. Dekker, and A. W. Einerhand.** 2003. Changes in small intestinal homeostasis, morphology, and gene expression during rotavirus infection of infant mice. J. Virol. **77:**13005–13016.
11. **Brown, G. R., G. Lindberg, J. Meddings, M. Silva, B. Beutler, and D. Thiele.** 1999. Tumor necrosis factor inhibitor ameliorates murine intestinal graft-versus-host disease. Gastroenterology **116:**593–601.
12. **Brown, G. R, and D. L. Thiele.** 2000. T-cell activation and differentiation are regulated by TNF during murine DBA/2→B6D2F1 intestinal graft-versus-host disease. J. Clin. Immunol. **20:**379–388.
13. **Cliffe, L. J., N. E. Humphreys, T. E. Lane, C. S. Potten, C. Booth, and R. K. Grencis.** 2005. Accelerated intestinal epithelial cell turnover: a new mechanism of parasite expulsion. Science **308:**1463–1465.
14. **Ellison, C. A., S. A. Natuik, A. R. Mcintosh, S. A. Scully, D. M. Danilenko, and J. G. Gartner.** 2003. The role of Interferon gamma, nitric oxide and lipopolysaccharide in intestinal graft-versus-host disease developing in F$_1$ hybrid mice. Immunology **109:**440–449.
15. **Else, K. J., F. D. Finkelman, C. R. Maliszewski, and R. K. Grencis.** 1994. Cytokine-mediated regulation of chronic intestinal helminth infection. J. Exp. Med. **179:**347–351.
16. **Else, K. J., D. Wakelin, D. L. Wassom, and K. M. Hauda.** 1990. The influence of genes mapping within the major histocompatibility complex on resistance to *Trichuris muris* infections in mice. Parasitology 101(Pt. **1:**61–67.
17. **Faulkner, H., N. Humphreys, J. C. Renauld, J. Van Snick, and R. Grencis.** 1997. Interleukin-9 is involved in host protective immunity to intestinal nematode infection. Eur. J. Immunol. **27:**2536–2540.
18. **Fish, S. M., R. Proujansky, and W. W. Reenstra.** 1999. Synergistic effects of interferon gamma and tumour necrosis factor alpha on T84 cell function. Gut **45:**191–198.
19. **Garside, P., R. K. Grencis, and A. M. Mowat.** 1992. T lymphocyte dependent enteropathy in murine *Trichinella spiralis* infection. Parasite Immunol. **14:**217–225.
20. **Gitter, A. H., K. Bendfeldt, J. D. Schulzke, and M. Fromm.** 2000. Leaks in the epithelial barrier caused by spontaneous and TNF-alpha-induced single-cell apoptosis. FASEB J. **14:**1749–1753.
21. **Grell, M., P. Scheurich, A. Meager, and K. Pfizenmaier.** 1993. TR60 and TR80 tumor necrosis factor (TNF) receptors can independently mediate cytolysis. Lymphokine Cytokine Res. **12:**143–148.
22. **Grell, M., G. Zimmermann, D. Hulser, K. Pfizenmaier, and P. Scheurich.** 1994. TNF receptors TR60 and TR80 can mediate apoptosis via induction of distinct signal pathways. J. Immunol. **153:**1963–1972.
23. **Guy-Grand, D., J. P. DiSanto, P. Henchoz, M. Malassis-Seris, and P. Vassalli.** 1998. Small bowel enteropathy: role of intraepithelial lymphocytes and of cytokines (IL-12, IFN-gamma, TNF) in the induction of epithelial cell death and renewal. Eur. J. Immunol. **28:**730–744.
24. **Guy-Grand, D., and P. Vassalli.** 1986. Gut injury in mouse graft-versus-host reaction: study of its occurrence and mechanisms. J. Clin. Investig. **77:**1584–1595.
25. **Heine, J., H. W. Moon, and D. B. Woodmansee.** 1984. Persistent cryptosporidium infection in congenitally athymic (nude) mice. Infect. Immun. **43:**856–859.
26. **Heller, R. A., K. Song, N. Fan, and D. J. Chang.** 1992. The p70 tumor necrosis factor receptor mediates cytotoxicity. Cell **70:**47–56.
27. **Helmby, H., K. Takeda, S. Akira, and R. K. Grencis.** 2001. Interleukin (IL)-18 promotes the development of chronic gastrointestinal helminth infection by downregulating IL-13. J. Exp. Med. **194:**355–364.
28. **Ijiri, K., and C. S. Potten.** 1983. Response of intestinal cells of differing

topographical and hierarchical status to ten cytotoxic drugs and five sources of radiation. Br. J. Cancer **47:**175–185.

29. **Li, Y. Q., C. Y. Fan, P. J. O'Connor, D. J. Winton, and C. S. Potten.** 1992. Target cells for the cytotoxic effects of carcinogens in the murine small bowel. Carcinogenesis **13:**361–368.

30. **Li, C. K. F., R. Seth, T. Gray, R. Bayston, Y. R. Mahida, and D. Wakelin.** 1998. Production of proinflammatory cytokines and inflammatory mediators in human intestinal epithelial cells after invasion by *Trichinella spiralis*. Infect. Immun. **66:**2200–2206.

31. **Little, M. C., L. V. Bell, L. J. Cliffe, and K. Else.** 2005. The characterization of intraepithelial lymphocytes, lamina propria leukocytes, and isolated lymphoid follicles in the large intestine of mice infected with the intestinal nematode parasite *Trichuris muris*. J. Immunol. **175:**6713–6722.

32. **MacDonald, T. T., and J. Spencer.** 1988. Evidence that activated mucosal T cells play a role in the pathogenesis of enteropathy in human small intestine. J. Exp. Med. **167:**1341–1349.

33. **McClane, S. J., and J. L. Rombeau.** 1999. Cytokines and inflammatory bowel disease: a review. JPEN J. Parenteral Enteral Nutr. **23:**S20–S24.

34. **Merger, M., J. L. Viney, R. Borojevic, D. Steele-Norwood, P. Zhou, D. A. Clark, R. Riddell, R. Maric, E. R. Podack, and K. Croitoru.** 2002. Defining the roles of perforin, Fas/FasL, and tumour necrosis factor alpha in T-cell induced mucosal damage in the mouse intestine. Gut **51:**155–163.

35. **Merritt, A. J., C. S. Potten, A. J. Watson, D. Y. Loh, K. Nakayama, K. Nakayama, and J. A. Hickman.** 1995. Differential expression of bcl-2 in intestinal epithelia. Correlation with attenuation of apoptosis in colonic crypts and the incidence of colonic neoplasia. J. Cell Sci. **108**(Pt. 6)**:**2261–2271

36. **Monteleone, G., and T. T. MacDonald.** 2000. Manipulation of cytokines in the management of patients with inflammatory bowel disease. Ann. Med. **32:**552–560.

37. **Mowat, A. M., and A. Ferguson.** 1982. Intraepithelial lymphocyte count and crypt hyperplasia measure the mucosal component of the graft-versus-host reaction in mouse small intestine. Gastroenterology **83:**417–423.

38. **Ossina, N. K., A. Cannas, V. C. Powers, P. A. Fitzpatrick, J. D. Knight, J. R. Gilbert, E. M. Shekhtman, L. D. Tomei, S. R. Umansky, and M. C. Kiefer.** 1997. Interferon-gamma modulates a p53-independent apoptotic pathway and apoptosis-related gene expression. J. Biol. Chem. **272:**16351–16357.

39. **Potten, C. S., C. Booth, and D. M. Pritchard.** 1997. The intestinal epithelial stem cell: the mucosal governor. Int. J. Exp. Pathol. **78:**219–243.

40. **Potten, C. S., and J. H. Hendry.** 1985. The microcolony assay in mouse small intestine, p. 155–159. *In* C. S. Potten and J. H. Hendry (ed.), Cell clones: manual of mammalian cell techniques. Churchill-Livingstone, Edinburgh, Scotland.

41. **Potten, C. S., J. W. Wilson, and C. Booth.** 1997. Regulation and significance of apoptosis in the stem cells of the gastrointestinal epithelium. Stem Cells **15:**82–93.

42. **Puddu, P., L. Fantuzzi, P. Borghi, B. Varano, G. Rainaldi, E. Guillemard, W. Malorni, P. Nicaise, S. F. Wolf, F. Belardelli, and S. Gessani.** 1997. IL-12 induces IFN-gamma expression and secretion in mouse peritoneal macrophages. J. Immunol. **159:**3490–3497.

43. **Ruemmele, F. M., S. Dionne, E. Levy, and E. G. Seidman.** 1999. TNFα-induced IEC-6 cell apoptosis requires activation of ICE caspases whereas complete inhibition of the caspase cascade leads to necrotic cell death. Biochem. Biophys. Res. Commun. **260:**159–166.

44. **Ruggiero, V., J. Tavernier, W. Fiers, and C. Baglioni.** 1986. Induction of the synthesis of tumor necrosis factor receptors by interferon-gamma. J. Immunol. **136:**2445–2450.

45. **Rutgeerts, P., G. Van Assche, and S. Vermeire.** 2004. Optimizing anti-TNF treatment in inflammatory bowel disease. Gastroenterology **126:**1593–1610.

46. **Schauer, D. B., and S. Falkow.** 1993. Attaching and effacing locus of a Citrobacter freundii biotype that causes transmissible murine colonic hyperplasia. Infect. Immun. **61:**2486–2492.

47. **Stuber, E., A. Buschenfeld, A. von Freier, T. Arendt, and U. R. Folsch.** 1999. Intestinal crypt cell apoptosis in murine acute graft versus host disease is mediated by tumour necrosis factor alpha and not by the FasL-Fas interaction: effect of pentoxifylline on the development of mucosal atrophy. Gut **5:**229–235.

48. **Stuber, E., A. Von Freier, D. Marinescu, and U. R. Folsch.** 1998. Involvement of OX40-OX40L interactions in the intestinal manifestations of the murine acute graft-versus-host disease. Gastroenterology **115:**1205–1215.

49. **Symons, L. E.** 1965. Kinetics of the epithelial cells, and morphology of villi and crypts in the jejunum of the rat infected by the nematode *Nippostrongylus brasiliensis*. Gastroenterology **49:**158–168.

50. **Tartaglia, L. A., M. Rothe, Y. F. Hu, and D. V. Goeddel.** 1993. Tumor necrosis factor's cytotoxic activity is signaled by the p55 TNF receptor. Cell **73:**213–216.

51. **Thiele, D. L., M. L. Eigenbrodt, S. E. Bryde, E. H. Eigenbrodt, and P. E. Lipsky.** 1989. Intestinal graft-versus-host disease is initiated by donor T cells distinct from classic cytotoxic T lymphocytes. J. Clin. Investig. **84:**1947–1956.

52. **Wakelin, D.** 1967. Acquired immunity to *Trichuris muris* in the albino laboratory mouse. Parasitology **57:**515–524.

53. **Wang, J., and Y. X. Fu.** 2005. Tumor necrosis factor family members and inflammatory bowel disease. Immunol. Rev. **204:**144–155.

54. **Wherry, J. C., R. D. Schreiber, and E. R. Unanue.** 1991. Regulation of gamma interferon production by natural killer cells in SCID mice: roles of tumor necrosis factor and bacterial stimuli. Infect. Immun. **59:**1709–1715.

55. **Yang, H., Y. Fan, and D. H. Teitelbaum.** 2003. Intraepithelial lymphocyte-derived interferon-gamma evokes enterocyte apoptosis with parenteral nutrition in mice. Am. J. Physiol. Gastrointest. Liver Physiol. **284:**G629–G637.